J Inf Process Syst, Vol.11, No.1, pp.134~147, March 2015
http://dx.doi.org/10.3745/JIPS.02.0016

ISSN 1976-913X (Print)
ISSN 2092-805X (Electronic)

JOURNAL OF INFORMATION PROCESSING SYSTEMS JIPS

Spatial Interpolation of Meteorologic Variables in Vietnam using the Kriging Method

Xuan Thanh Nguyen*, Ba Tung Nguyen*, Khac Phong Do*, Quang Hung Bui*, Thi Nhat Thanh Nguyen*, Van Quynh Vuong**, and Thanh Ha Le*

Abstract

This paper presents the applications of Kriging spatial interpolation methods for meteorologic variables, including temperature and relative humidity, in regions of Vietnam. Three types of interpolation methods are used, which are as follows: Ordinary Kriging, Universal Kriging, and Universal Kriging plus Digital Elevation model correction. The input meteorologic data was collected from 98 ground weather stations throughout Vietnam and the outputs were interpolated temperature and relative humidity gridded fields, along with their error maps. The experimental results showed that Universal Kriging plus the digital elevation model correction method outperformed the two other methods when applied to temperature. The interpolation effectiveness of Ordinary Kriging and Universal Kriging were almost the same when applied to both temperature and relative humidity.

Keywords

Interpolation, Meteorologic Variables, Kriging

1. Introduction

Temperature and humidity are the two main meteorologic variables that directly impact physical and biological processes. Knowledge of the spatial temporal variability of climatic conditions is required for assessing the recent climate change and greenhouse effect [1]. Spatially and temporally continuous gridded meteorologic datasets are important in many applications, such as in forest fire risk modeling, soil sciences, and ecological studies [2,3]. However, the weather station network is often sparse and meteorologic data may not be available where it is most needed. Various interpolation methods have been developed to generate the grid dataset of interest meteorologic variables. The purpose is to predict meteorologic values based on the spatial autocorrelation among observations and possibly ancillary variables for locations where no actual observations are available.

Various statistical methods have been developed for interpolating climate data. Many studies have pointed out that Kriging interpolation methods have high accuracy and low bias compared with other geo-

Manuscript received November 14, 2014; accepted January 19, 2015.
Corresponding Author: Le Thanh Ha (ltha@vnu.edu.vn)
* University of Engineering and Technology, Vietnam National University, Hanoi, Vietnam (thanhnx_1@vnu.edu.vn, {tungnb, phongdk, hungbq, thanhntn}@fimo.edu.vn, ltha@vnu.edu.vn)
** Vietnam Forestry University, Hanoi, Vietnam (quynhxm_2005@yahoo.com)

statistical methods [4,5]. These methods are a linear combination of weights, which are determined by the spatial variation structure [6]. Previously, some papers implemented Kriging methods on their country-level data. In [7], 922 meteorological stations in the United States were interpolated using Residual Kriging plus elevation and 12 directions models. Another paper applied a Kriging method with an external drift (e.g., mean elevation, sea, and lake percentage) to station-based temperature and precipitation in Finland [6]. In [8-10], they produced monthly, min, max, and average climate gridded datasets from their country-level ground weather stations using Kriging methods. In Vietnam, there has been some research carried out on Kriging interpolation on frost and low temperature data from stations, MODIS, and NOAA data from the northwest region of the country. In [11,12], a 100×100 m^2 high-resolution warning map of frost and low temperatures was constructed and continuously updated in some provinces.

This research targets were used to develop interpolation models for generating temperature and relative humidity gridded fields from scattered ground station observations. We proposed three models including Ordinary Kriging (OrK), Universal Kriging (UnK), UnK plus Digital Elevation Model (UnK+DEM). The models were then applied to ten years of 98 ground weather stations data in Vietnam, plus satellite images as ancillary data. Then, ten-fold cross-validation was used to compare these three models and choose to the best one, which was the UnK+DEM.

The paper consists of four main sections, which are the introduction, datasets and methodology, results, and the conclusion.

2. Datasets and Methodology

2.1 Study Area

The study area for this research was in Vietnam, which is located at approximately 8°N to 23°N and 110°E to 120°E (See Fig. 1). Vietnam is a tropical country and spans a land area of around 33 million ha, of which 13.9 million ha are forests (3.5 million ha of forest plantations and 10.4 million ha of natural forests). Vietnam is divided into eight administration regions: Northwest, Northeast, Red River Delta, North-Central Coast, South-Central Coast, Central Highlands, Southeast, and the Mekong River Delta.

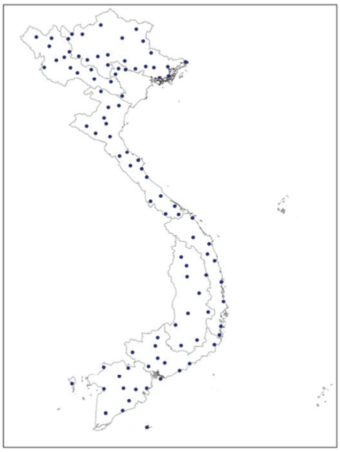

Fig. 1. Weather stations map in Vietnam.

2.2 Datasets

There are two types of data that were collected and used in this study.

Ground station data: all meteorologic data was collected from the Forest Protection Department, Vietnam Administration of Forestry from 2004 to 2014. This meteorologic data included temperature (GR TEMP) and relative humidity (GR RH) measured at 13:00 every day from 98 stations located throughout Vietnam, as seen in Fig. 1. In addition, spatial information, including the location and altitude (GRA) of these ground stations, were also included in the data set.

Satellite Digital Elevation Model (DEM), ASTER, is a medium-to-high spatial resolution, multispectral imaging system that flies onboard the TERRA satellite. The imaging system acquires stereoscopic images at a spatial resolution of 15 m for deriving DEM. As a result, ASTER DEM is a 30-m elevation dataset that was created by stereo-correlating automated techniques [13]. In this work, ASTER-DEM is used as ancillary data for the removal of the elevation effect of temperature data.

2.3 Methodology

2.3.1 Kriging spatial interpolation for meteorologic data

In this section, we present the application of Kriging spatial interpolation methods to temperature and humidity. This spatial interpolation is applied to temperature and humidity variables independently. For simplicity, meteorologic variable terminology is used to indicate either the temperature variable or humidity variable.

The output of interpolation consists of interpolated meteorologic fields in Vietnam and their error maps. Kriging works well in cases when the statistical assumptions are met and in cases where there are a sufficient number of non-clustered target observations. As such, the spatial pattern (covariance) can be described with statistical significance and with a relatively sufficient level of detail in connection to the spatial gradients of variation of the target variable [14]. The meteorologic data, which is comprised of years of data from 98 ground stations, is suitable for applying Kriging interpolation.

All interpolation algorithms estimate the destination value at a given location as a weighted sum of data values at surrounding locations. Kriging estimates the spatial variation structure through a variogram and takes the spatial autocorrelation into consideration [15]. The Kriging estimator is modeled as the sum of a global trend μ (measuring broad trends in the data over the entire study region) and a local stochastic variation ϵ [16]:

$$Z(s) = \mu(s) + \epsilon(s) \tag{1}$$

where s denotes the spatial coordinate. Based on the assumptions of the global trend μ, many types of Kriging methods have been derived. For example, Simple Kriging (SK) assumes $= 0$; Ordinary Kriging (OK) assumes the unknown constant mean; and Universal Kriging (UK) assumes a general polynomial trend as follows:

$$z = ax + by + c \tag{2}$$

where x, y, are the variables for the x-latitude and y-longitude, respectively, z is statistically analyzed from past data. To avoid seasonal side effects, we estimated z from the monthly data. The regression model (2) can be seen as a mathematical plane that fits a set of 3-dimensional points (x, y, z). An example of a temperature trend function is illustrated in Fig. 2(a). It demonstrates the variation of temperatures observed on January 10, 2012 when increasing latitude over all of Vietnam, as shown in Fig. 2(b).

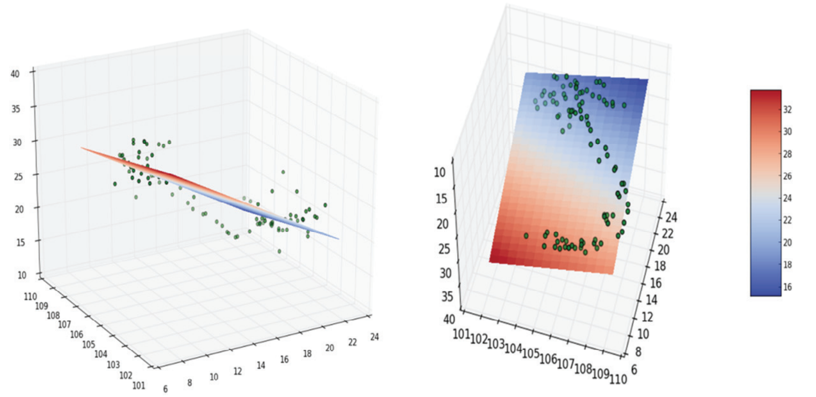

(a) (b)

Fig. 2. Visualization of trend function on January 10, 2012. (a) Temperature trend function, (b) the variation of temperatures according to the latitude.

Many regionalized variables show local trends or even broader regional trends when spatially analyzed. Trends may be caused by natural processes that are related to directions (i.e., the effect of progressively increasing the latitude and other well-known dependencies between surface temperature and elevation [17-19]). A non-stationary regionalized variable contains two components, which are known as drift (or trend) and residual. The drift represents the spatial trend inherent in the data and the residual is the difference between the real value and the drift. First, the UK removes the drift component from a regionalized variable so that the residuals will be more stationary. The drift is estimated by a regression model which is a mathematical function that represents data trends. After wrapping up elimination, the variogram model of the residual is calculated and interpolated to obtain the elementary residual result. Finally, the drift is returned back to the estimated residuals to obtain the final interpolated value.

The unknown meteorologic random variable $Z(s_0)$ at spatial location s_0 is expressed as weighted linear combinations of the available meteorologic samples:

$$Z_{s_0} = \sum_{i=1}^{N} \omega_{s_i} . Z_{s_i} \tag{3}$$

where:

$$\sum_{i=1}^{N} \omega_{s_i} = 1 \tag{4}$$

N is the number of ground stations around s_0, and $Z(s_i)$ is the meteorologic observation at station s_i associated with weight w_{si}. This method attempts to determine weights, w_{si}, in order to minimize the Kriging error σ_r^2, which is defined as follows:

$$\begin{aligned}\sigma_r^2 &= Var\left(\bar{Z}_{s_0} - Z_{s_0}\right) \\ &= \sigma^2 + \sum_{i=1}^{N}\sum_{j=1}^{N} \omega_{s_i}\,\omega_{s_j}\,\bar{C}_{s_{ij}} \\ &-2\sum_{i=1}^{N} \omega_{s_i}\bar{C}_{s_{i0}}\,,\end{aligned} \tag{5}$$

where σ^2 is the covariance of the random variable $Z(s_0)$ with itself and we assume that all of our random variables have the same variance. $\bar{C}_{s_{ij}}$ is the covariance between two observed meteorologic samples at locations s_i and s_j. The corresponding problem can be represented as follows:

$$\begin{aligned}&\text{Minimize } \sigma^2 + \sum_{i=1}^{N}\sum_{j=1}^{N} \omega_{s_i}\,\omega_{s_j}\,\bar{C}_{s_{ij}} - 2\sum_{i=1}^{N} \omega_{s_i}\bar{C}_{s_{i0}} \\ &\text{Subject to } \sum_{\mathrm{i}=1}^{\mathrm{N}} \omega_{\mathrm{s_i}} = 1\end{aligned} \tag{6}$$

Solving the optimization problem (7) results in Kriging system:

$$\begin{bmatrix}\bar{C}_{s_{10}}\\ \bar{C}_{s_{20}}\\ \vdots \\ \bar{C}_{s_{N0}}\\ 1\end{bmatrix} = \begin{bmatrix}\bar{C}_{s_{11}} & \bar{C}_{s_{12}} & \cdots & \bar{C}_{s_{1N}} & 1\\ \bar{C}_{s_{21}} & \bar{C}_{s_{22}} & \cdots & \bar{C}_{s_{2N}} & 1\\ \vdots & \vdots & \ddots & \vdots & \vdots\\ \bar{C}_{s_{N1}} & \bar{C}_{s_{N2}} & \cdots & \bar{C}_{s_{NN}} & 1\\ 1 & 1 & \cdots & 1 & 0\end{bmatrix} \cdot \begin{bmatrix}\omega_{s_1}\\ \omega_{s_2}\\ \vdots \\ \omega_{s_N}\\ \lambda\end{bmatrix} \tag{7}$$

where λ is the Lagrange multiplier for error minimization.

The covariances are retrieved from a variogram model, which represents the spatial correlation of the target variable as follows:

$$\bar{C}_{s_{ij}} = \sigma^2 - \gamma(h) \tag{8}$$

where h is the distance between stations s_i and s_j, and the model $\gamma(h)$ is constructed from scatter experimental point sets. These points are defined by calculating the semivariance and distance between all possible pairs of values in the region of interest. Several models can be used to fit these points, such as Gaussian, Spherical, and Exponential [20,21]. Then, the best-suited one is selected by comparing the mean square error between the variogram model and experimental data. The construction of the variogram model used in this work is explained in the next section.

Based on the variogram model, the interpolation error at location s_0 can be calculated in terms of the standard deviation as follows:

$$\bar{E}(s_0) = \sum_{i=1}^{N} \omega_{s_i} \gamma(h_{i0}) \tag{9}$$

where h_{i0} is the distance between locations s_i and s_0.

2.3.2 Elevation correction for temperature

It was shown in [22] that temperature decreases with altitude at approximately 6.5°C per km. A normalization process must be applied to the GR TEMP to compensate for the altitude affects before interpolation. In this work, a constant coefficient obtained from the relationship between temperature and elevation was applied to transform the GR TEMP to a zero-level elevation temperature (equivalent temperature at sea level) as follows:

$$T_0 = T_{GR} - 0.0065 \times ALT_{GR} \tag{10}$$

where T_{GR} is the observed ground station temperature and ALT_{GR} is the station altitude in meters.

2.3.3 ASTER DEM calibration

All of the DEM of Vietnam is clipped from ASTER-DEM dataset. In order to incorporate ASTER-DEM as the ancillary data for the spatial meteorologic data interpolation, a calibration process must be applied to the ASTER-DEM data using ground truth. In this research, ground station altitude (GRA) is used as the ground truth for ASTER-DEM calibration in the region of Vietnam. Experimental results show that the correlation (R^2) between GRA and ASTER DEM is about 0.59.

2.3.4 Ten-fold cross validation

Cross validation is used to assess and choose the best interpolation methods, including the results from OrK, UnK, and UnK+DEM. A study of cross validation indicates that for real word datasets, the best method to use for model selection is ten-fold cross validation, even if computation power allows using more folds. The advantage of this method is that all observations are used for both training and validation, and each observation is used for validation exactly once [23].

In this research, the interpolated meteorologic data are applied to ten-fold cross validation, in which, 98 ground stations are randomly partitioned into ten subsets equally. A single subset is retained as the validation data for testing, and the nine remaining others are used as interpolation data. The cross-validation process is then repeated 10 times, with each of the ten subsets used exactly once as the validation data. The 10 results from the folds are then averaged to produce a final estimation. The relative precision of the three models was then compared in terms of mean error (ME) and mean square error (MSE).

3. Results and Discussions

3.1 Spatial Correlation and Variogram Modeling

The spatial correlation of the regionalized variable helps to build the variogram needed for Kriging interpolation, as stated in the previous section. In this section, we demonstrate the experimental results of the spatial correlation for temperature and humidity observed at 98 ground stations.

With each type of meteorologic data, the correlation coefficient (R^2) and distance (D) was estimated between each pair of observed data. In particular, 98 ground stations have 98×97 pairs of two distinguishable stations s_i and s_j. The correlation coefficient and the distance between s_i and s_j can be estimated from 10-year of meteorologic data and stations spatial information. A pair of stations (s_i, s_j) is featured by correlation ${R_{ij}}^2$ and distance D_{ij}. For representing the spatial correlation between all pairs of ground stations meteorologic datasets, we plotted these calculated datasets on a spatial correlation graph with D_{ij} on the X-axis and ${R_{ij}}^2$ on the Y-axis. For visualization, the average of ${R_{ij}}^2$ is taken at every quantized distance value with quantization parameter $d = 50$ km. This averaged and quantized data is plotted on the average spatial correlation graph.

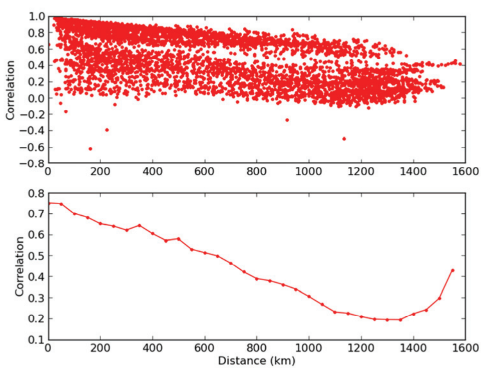

Fig. 3. Spatial correlation of temperature respect to distance.

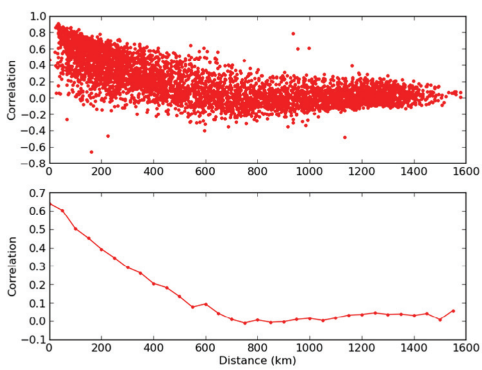

Fig. 4. Spatial correlation of humidity respect to distance.

Fig. 3 depicts the spatial correlation graph (upper) and average correlation graph (lower) of the temperatures measured at 98 meteorologic ground stations in Vietnam. It can be seen that the spatial correlation of the temperature variable slowly decreases when distance increases. High correlations (higher than 0.4) of temperature between two stations 700 km apart were still observed. Fig. 4 depicts the same humidity graphs. We can see that spatial correlation of humidity decreases faster than that of temperature when distance increases. High correlations of humidity between two stations 200 km apart were also observed.

From Figs. 3 and 4, we can observe a significant difference in the spatial correlation between temperature and humidity variables. Therefore, the number of neighbor ground stations N, as stated in (3) and (4), for each meteorologic variable is not the same. We once again plotted the spatial correlation of each meteorologic variable with respect to the number of neighboring ground stations.

Fig. 5 depicts the spatial correlation graph (upper) and average correlation graph (lower) with respect to the number of neighboring ground stations. It can be seen that the spatial correlation of temperature variable decrease slowly when the number of neighbors increases. High correlations (higher than 0.7) are observed when the number of neighbors is less than 10. Therefore, we use $N_T = 10$ for the number of neighboring ground stations when interpolating the temperature variable. Fig. 6 depicts the humidity graphs. High correlations (higher than 0.6) are observed when the number of neighbors is less than 5.

Therefore, we use $N_H = 5$ for the number of neighboring ground stations when interpolating the humidity variable.

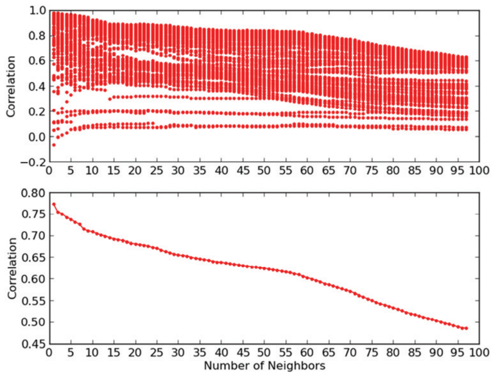

Fig. 5. Spatial correlation of temperature respect to number neighbor ground stations.

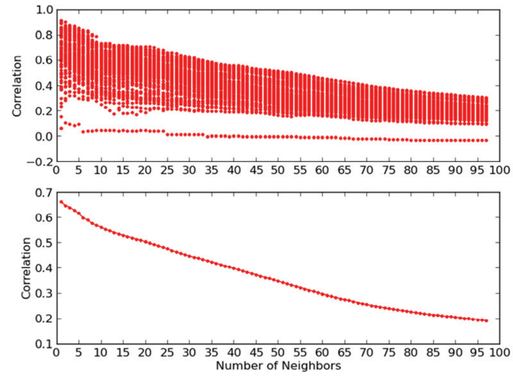

Fig. 6. Spatial correlation of humidity respect to number of neighbor ground stations.

As stated in the previous section, covariance $\bar{C}_{s_{ij}}$ can be retrieved from a variogram model in (8), which is constructed from scatter experimental point sets. These points are calculated from the semi-variance and distance between all possible pairs of ground stations in the period time of interest. In this work, one month before observation day is used for obtaining z value. Several models, such as Gaussian, Spherical, and Exponential, which fit these points were used. We observed from the experimental results that the Spherical model is the best fit in terms of comparing the mean square error between the variogram model and experimental data. The spherical model is explained as follows:

$$\hat{\gamma}(h) = \begin{cases} c_0 + c_1\left[\frac{3}{2}\frac{h}{a_0} - \frac{1}{2}\left(\frac{h}{a_0}\right)^3\right] & , h \le a_0 \\ c_0 + c_1 & , h > a_0 \end{cases} \tag{11}$$

where c_0 is the nugget, $c_0 + c_1$ is sill, and a_0 is the practical range, as visualized in Fig. 7.

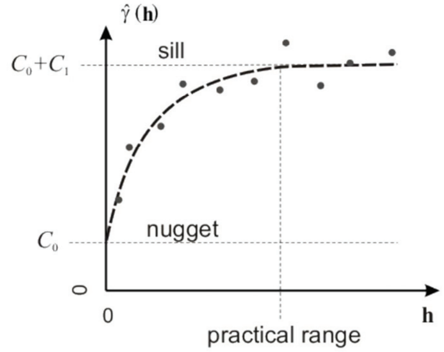

Fig. 7. Visualization of Spherical model.

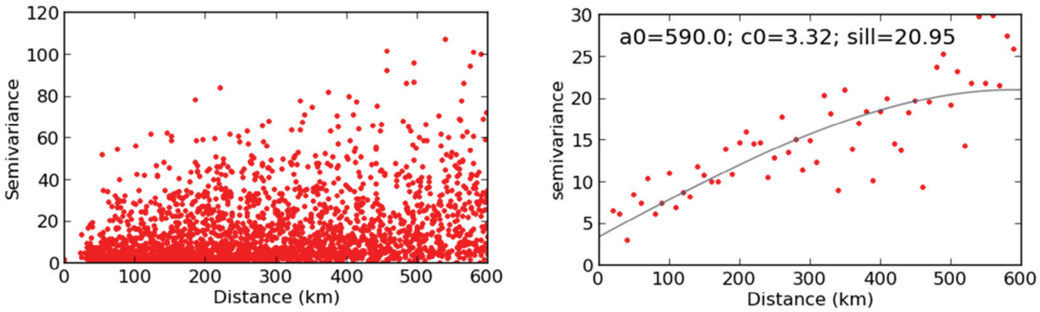

Fig. 8. An example of Spherical model fitted to one month temperature data before March 16, 2012.

Fig. 8 depicts an example of Spherical model fitted to one month of temperature data before March 16, 2012. The upper graph shows the point sets and the lower graph shows the Spherical model fitted to the average value of point sets at every 10 km distance. We can see that the practical range of temperature is about 590 km. Fig. 9 depicts the same information as in Fig. 8 of the Spherical model fitted to one month's worth of humidity data before February 20, 2012. We can see that the practical range of humidity is about 282 km.

In order to apply the Kriging interpolation to meteorologic variables observed from 98 ground stations at any given day, one month's worth of meteorologic data before that day was used to construct Spherical model. Finally, the covariance matrix was calculated by using Eq. (8).

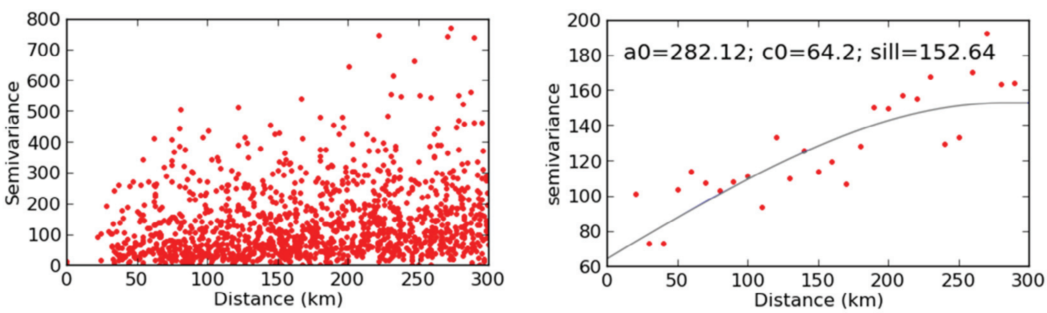

Fig. 9. An example of Spherical model fitted to one month humidity data before February 20, 2012.

3.2 Ten-fold Cross-Verification Results

In order to evaluate the effectiveness of the interpolation methods, we used the root mean square error (RMSE), which is defined as follows:

$$RMSE = \frac{1}{T} \cdot \sum_{t=1}^{T} \left(sqrt \left(\frac{1}{M} \cdot \sum_{i=1}^{M} \left(Z_{s_i} - \bar{Z}_{s_i} \right)^2 \right) \right) \tag{12}$$

and mean percentage error (MPE), which is defined as follows:

$$MPE = \frac{1}{T} \cdot \sum_{t=1}^{T} \left(\frac{1}{M} \cdot \sum_{i=1}^{M} \frac{\left| Z_{s_i} - \bar{Z}_{s_i} \right|}{Z_{s_i}} \cdot 100\% \right) \tag{13}$$

where M is the number of testing stations T is the number of tests in a ten-fold estimation; Z_{s_i} and $\bar{Z}_{s_i}$ are the observed meteorologic variables and its interpolated value, respectively.

Table 1. Temperature models validation results

Model	RMSE (°K)	MPE (%)
OrK	2.195	0.522
UnK	2.192	0.523
UnK+DEM	2.026	0.509

OrK = Ordinary Kriging, UnK = Universal Kriging, DEM = Digital Elevation Model, RMSE = root mean square error, MPE = mean percentage error.

Table 2. Relative humidity models validation results

Model	RMSE (%)	MPE (%)
OrK	7.155	8.434
UnK	7.119	8.398

OrK=Ordinary Kriging, UnK=Universal Kriging, RMSE = root mean square error, MPE = mean percentage error.

Table 1 shows the validation results of temperature interpolation. It can be seen from the table that the interpolation errors of OrK are almost the same as those of UnK methods. UnK errors are the smallest with RMSE at 2.026°K and with MPE they are 0.509%. Table 2 shows the validation results of relative humidity interpolation. Here, ASTER DEM is not used in interpolation. It can also be seen from this table that the interpolation errors of UnK are slightly lower than those of OrK.

3.3 Interpolation Results

Figs. 10 and 11 depict the interpolated temperature field 0.1°×0.1° and its interpolation error map on November 23, 2013 using UnK+DEM. The temperature gradually increases from the North to the South of Vietnam, which reflects the latitude temperature affects. It can be seen from Fig. 10 that the effects of altitude on mountainous regions (Northwest and Central Highlands) are different from those on the delta regions (Red River Delta and Mekong River Delta). Sudden changes in temperature are found in mountainous regions and smooth temperature gradients are found in delta regions. Fig. 11 shows the interpolation error map in terms of the standard deviation defined in (9). This figure reveals the interpolation error spatially. A minimal amount of interpolation errors were observed at and nearby ground station regions (white spots) and they increase as the distance to the nearest ground station increases (black regions).

Figs. 12 and 13 depict the interpolated relative humidity field 0.1°×0.1° and its interpolation error map on November 23, 2013 using UnK. In Fig. 12, the spreading of high values of humidity from the Northeast down to the midland region may be because of a monsoon at that time. Fig. 13 reveals the interpolation error spatially in terms of standard derivation defined in (9).

4. Conclusion

This paper contributes to the literature on interpolation algorithms and meteorologic data processing by developing a Kriging model for interpolating meteorologic variables in Vietnam. Temperature and relative humidity data from ground stations in Vietnam were spatially interpolated using Kriging techniques. Three different types of Kriging methods, including OrK, UnK, and UnK+DEM, were used for interpolation. The ten-fold verification results show that UnK+DEM is the best model as it has the smallest error for temperature interpolation, whereas OrK and UnK are the almost the same accuracy for both temperature and relative humidity.

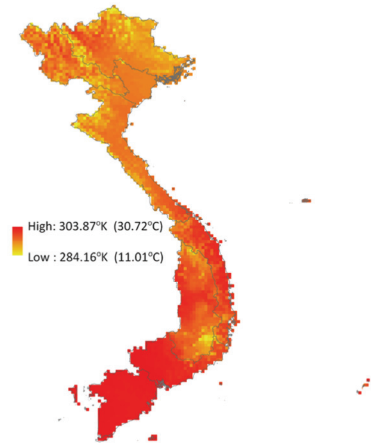

Fig. 10. Interpolated temperature field in Vietnam, November 23, 2013.

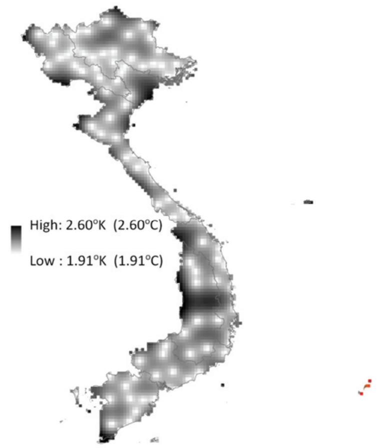

Fig. 11. Interpolation error map in Vietnam, November 23, 2013.

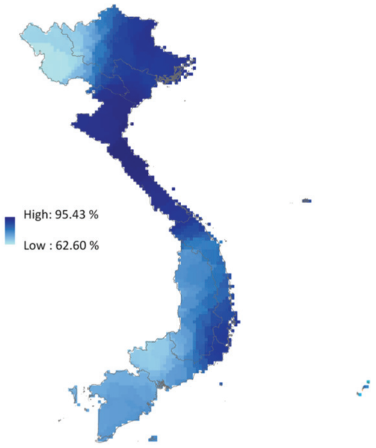

Fig. 12. Interpolated relative humidity field in Vietnam, November 23, 2013.

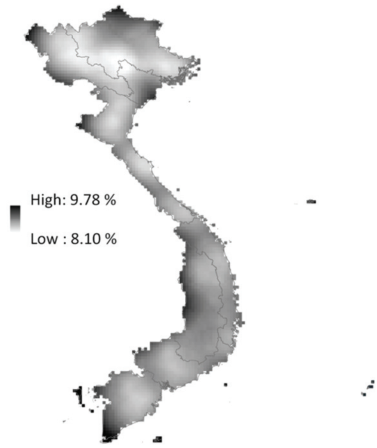

Fig. 13. Interpolation relative humidity error map in Vietnam, November 23, 2013.

Acknowledgement

This research was possible due to the funds received from the "Integration of WebGIS and multi-date and multi resolution satellite image processing technologies for forest fire monitoring in Vietnam, QGTD.12.25" project and from the "Forest fire information system, QGTD.13.26" project from Vietnam National University, Hanoi.

References

[1] M. B. Araújo and M. Luoto, "The importance of biotic interactions for modelling species distributions under climate change," *Global Ecology and Biogeography*, vol. 16, no. 6, pp. 743-753, 2007.

[2] J. Miller and J. Franklin, "Modeling the distribution of four vegetation alliances using generalized linear models and classification trees with spatial dependence," *Ecological Modelling*, vol. 157, no. 2, pp. 227-247, 2002.

[3] T. L. Liu, K. W. Juang, and D. Y. Lee, "Interpolating soil properties using kriging combined with categorical information of soil maps," *Soil Science Society of America Journal*, vol. 70, no. 4, pp. 1200-1209, 2006.

[4] X. Li, G. Cheng, and L. Lu, "Spatial analysis of air temperature in the Qinghai-Tibet Plateau," *Arctic, Antarctic, and Alpine Research*, vol. 37, no. 2, pp. 246-252, 2005.

[5] J. S. Yang, Y. Q. Wang, and P. V. August, "Estimation of land surface temperature using spatial interpolation and satellite-derived surface emissivity," *Journal of Environmental Informatics*, vol. 4, no. 1, pp. 37-44, 2004.

[6] J. Aalto, P. Pirinen, J. Heikkinen, and A. Venäläinen, "Spatial interpolation of monthly climate data for Finland: comparing the performance of kriging and generalized additive models," *Theoretical and Applied Climatology*, vol. 112, no. 1-2, pp. 99-111, 2013.

[7] T. Wu and Y. Li, "Spatial interpolation of temperature in the United States using residual kriging," *Applied Geography*, vol. 44, pp. 112-120, 2013.

[8] C. Daly, M. Halbleib, J. I. Smith, W. P. Gibson, M. K. Doggett, G. H. Taylor, J. Curtis, and P. P. Pasteris, "Physiographically sensitive mapping of climatological temperature and precipitation across the conterminous United States," *International Journal of Climatology*, vol. 28, no. 15, pp. 2031-2064, 2008.

[9] S. P. Serbin and C. J. Kucharik, "Spatiotemporal mapping of temperature and precipitation for the development of a multidecadal climatic dataset for Wisconsin," *Journal of Applied Meteorology and Climatology*, vol. 48, no. 4, pp. 742-757, 2009.

[10] R. Benavides, F. Montes, A. Rubio, and K. Osoro, "Geostatistical modelling of air temperature in a mountainous region of Northern Spain," *Agricultural and Forest Meteorology*, vol. 146, no. 3, pp. 173-188, 2007.

[11] D. V. Kham, H. D. Cuong, and N. T. Giang, "Study for building a frost and low temperature monitoring and warning model for north west region in Vietnam," in *Proceedings of the National Scientific Conference on Meteorology and Hydrology, Environment and Climate Change*, 2012, pp. 161-167.

[12] D. V. Kham, T. T. Tam, N. H. Quyen, and N. H. Son, "Method of construction zoning map of frost and low temperature in the northwest of Vietnam," in *Proceedings of the National Scientific Conference on Meteorology and Hydrology, Environment and Climate Change*, 2012, pp. 168-174.

[13] A. Hirano, R. Welch, and H. Lang, "Mapping from ASTER stereo image data: DEM validation and accuracy assessment," *ISPRS Journal of Photogrammetry and Remote Sensing*, vol. 57, no. 5, pp. 356-370, 2003.

[14] G. Mulugeta, "Manual and automated interpolation of climatic and geomorphic statistical surfaces: an evaluation," *Annals of the Association of American Geographers*, vol. 86, no. 2, pp. 324-342, 1996.

[15] D. Hattis, Y. Ogneva-Himmelberger, and S. Ratick, "The spatial variability of heat-related mortality in Massachusetts," *Applied Geography*, vol. 33, pp. 45-52, 2012.

[16] G. Matheron, *Le Krigeage Universel*. Paris: École Nationale Supérieure des Mines de Paris, 1969.

[17] S. H. Chua and R. L. Bras, "Optimal estimators of mean areal precipitation in regions of orographic influence," *Journal of Hydrology*, vol. 57, no. 1, pp. 23-48, 1982.

[18] S. L. Dingman, D. M. Seely-Reynolds, and R. C. Reynolds, "Application of kriging to estimating mean annual precipitation in a region of orographic influence1," *Journal of the American Water Resources Association*, vol. 24, no. 2, pp. 329-339, 1988.

[19] D. L. Phillips, J. Dolph, and D. Marks, "A comparison of geostatistical procedures for spatial analysis of precipitation in mountainous terrain," *Agricultural and Forest Meteorology*, vol. 58, no. 1, pp. 119-141, 1992.

[20] M. Armstrong and R. Jabin, "Variogram models must be positive-definite," *Mathematical Geology*, vol. 13, no. 5, pp. 455-459, 1981.

[21] N. Cressie, "Fitting variogram models by weighted least squares," *Journal of the International Association for Mathematical Geology*, vol. 17, no. 5, pp. 563-586, 1985.

[22] C. Rolland, "Spatial and seasonal variations of air temperature lapse rates in Alpine regions," *Journal of Climate*, vol. 16, no. 7, pp. 1032-1046, 2003.

[23] R. Kohavi, "A study of cross-validation and bootstrap for accuracy estimation and model selection," in *Proceedings of the International Joint Conference on Artificial Intelligence (IJCAI)*, Montreal, Canada, 1995, pp. 1137-1145.

Xuan Thanh Nguyen http://orcid.org/0000-0001-5464-0327

He received the B.S. in Computer Science from University of Engineering and Technology, Vietnam National University (UET, VNU), Hanoi, Vietnam in 2013. During 2013-2014, he studied first year of master program at UET, VNU and did research at Human Machine Interaction Laboratory, UET-VNU. Now, He is studying second year of master at Japan Advanced Institute of Science and Technology. His research interests include Computer Vision, Satellite Image Processing and Video Coding.

Ba Tung Nguyen http://orcid.org/0000-0002-3020-3058

He received the B.S. degree in Computer Science from University of Engineering and Technology (UET), VNU in 2013. After graduation, he works in Human-Machine Interaction Lab on a project about 'Human gestures recognition. And now he is undertaking a master course as a member of the Multidisciplinary Integrated Technologies Center For Field Monitoring at UET-VNU. His research interests include Human Gestures Recognition and Satellite Imagery Processing for Early Warning in Forest Fire.

Khac Phong Do http://orcid.org/0000-0002-6487-3420

He received the B.S. degree in Computer Science from University of Engineering and Technology, Vietnam National University, Hanoi (UET–VNU) in 2014. At the moment, he is enrolling a Master course as a member of Field Monitoring Center at UET–VNUHN. His current research interests consist of Satellite Image Processing, Meteorologic Data Interpolation.

Quang Hung Bui http://orcid.org/0000-0001-5250-4719

Bui Quang Hung received his B.Sc. from Vietnam National University in 2001. He received M.E. and Ph.D. from Division of Systems Science and Applied Informatics, Graduate School of Engineering Science, Osaka University in 2005 and 2008, respectively. Currently he is Director of the Multidisciplinary Integrated Technologies Center for Field Monitoring, Vietnam National University of Engineering and Technology. His research interests are Spatial Databases, Spatial Data Infrastructure, Spatial Data Mining and Geographical Information Systems.

Thi Nhat Thanh Nguyen http://orcid.org/0000-0002-7253-3813

She received B.S. and M.S. degrees in Information Technology from the College of Technology, Vietnam National University, Hanoi in 2005. She received a Ph.D. at University of Ferrara, Italy in 2012. Her research interests are in Satellite Image Processing, Air Pollution, and Satellite Aerosol. She is now a lecturer and researcher in University of Engineering and Technology, Vietnam National University.

Van Quynh Vuong http:// orcid.org/0000-0002-3375-3362

He received a Ph.D. degree in silviculture and forest fire management in 1991 at the Voronhezo Forestry University in the Republic of the Russian Federation. He has been a professor at Forestry University of Vietnam since 2012. His research interests are in the area of forest hydro-meteorology, forest fire management, environmental protection and disaster prevention. They include topics such as measures to use of forests to mitigate flooding and water resource stability, valuation of environmental services of forests, forest fire risk prediction, forest fire prevention, forest resources monitoring.

Thanh Ha Le http://orcid.org/0000-0002-7288-0444

Ha Le Thanh received B.S. and M.S. degrees in Information Technology from the College of Technology, Vietnam National University, Hanoi in 2005. He received a Ph.D. at the Department of Electronics Engineering at Korea University. In 2010, he joined the Faculty of Information Technology, University of Engineering and Technology, Vietnam National University, Hanoi as a lecturer and researcher. His research interests are multimedia processing, coding satellite image processing and computer vision. He is now doing research on forest fire using remote sensing approach as well as high efficient and multiview video coding.